CRYO/02/020
February 23,2002

A theoretical investigation on current imbalance in flat two layer superconducting cables

A. Akhmetov, L. Bottura, M. Breschi , P. L. Ribani

Distribution: Internal

Presented: Workshop on Computation of Thermo-Hydraulic Transients in Superconductors, Frascati, 6-9 September, 2000

Published: Cryogenics, **40**, 627-636, 2000

Summary

A model for the simulation of current distribution in superconducting Rutherford cables is described. The model assumes that interstrand currents can flow continuously among the strands, as if the contact resistances were smeared along the cable length. The model is aimed at the simulation of the generation and development of long range current loops in the presence of time dependent magnetic fields. The results of the model are compared with those obtained through the lumped constants circuit model currently used to calculate the current distribution in Rutherford cables obtaining a good quantitative agreement. The model has also been applied to the study of current distribution in the Rutherford cable of a short LHC dipole magnet. The calculated values of current differences among the strands are in qualitative agreement with experimental data on the amplitude of the periodic oscillations of the magnetic field in the magnet bore.

1. Introduction

Superconducting cables are made of a number of multifilamentary composites (strands) consisting of many superconducting filaments embedded in a matrix of normal metal. The strands are then twisted or transposed together to build the final cable. The application of current ramps or time dependent external fields to multistrand cables generates screening currents in both the superconducting filaments and the normal metal matrix. Several methods have been proposed to study the resulting eddy currents and the corresponding AC losses [1-3]. The study of these currents is beyond the scope of this work.

We focus our attention on the study of the eddy currents distribution which is induced by time dependent magnetic fields in the paths formed by the contacts between the different strands of the multistrand cable. These interstrand eddy currents are superimposed to the intrastrand eddy currents, but the approximation to study the two phenomena independently is widely accepted, because of the different time constants of the two current distributions.

Two main kinds of interstrand eddy currents can be distinguished, namely short and long range coupling currents. The last ones are often indicated as "Boundary Induced Coupling Currents" (BICC's) [4] or "Supercurrents" [5-7]. The short range coupling currents have a typical loop length equal to the cable twist pitch and exhibit time constants in the range from 0.01 to 1 s. The long range coupling currents can flow along the whole cable length, and have very high time constants, in the range from 10 to 10^5 s in practical cables. Their amplitude can be orders of magnitude higher than that of the short range coupling currents.

In the case of Rutherford cables, in which the strands are compressed to form a flat, two layers, cable, a network model has been developed to study the current distribution among the strands. One of the earliest presentations of this model was given by Morgan in 1973 [8], and assumes that the strands in one layer have electrical contacts with those in the other layer, but not between themselves. Morgan reports that “a direct application of Maxwell‘s equations to a flat metal-filled braid was attempted but dropped owing to the non isotropic structure of the cable”. For this reason he developed a lumped-constant circuit approach. In the Morgan’s model the Faraday’s and Kirchhoff’s equations are applied to all the loops formed by two adjacent strands of one layer crossing any two adjacent strands of the other layer. The braid is assumed to be infinitely long with uniform cross contact resistance and uniform field along the cable length, even if field variations across the cable width are allowed. In this way only N-1 independent loops have to be solved, where N is the total number of strands (see Fig. 1). The solution found for the cross over currents at an arbitrary position is then considered to be uniformly repeated along the cable length.

In more advanced versions of the network model [4, 9-13] the N-1 loops considered by Morgan become the components of the basic units for the calculation of the current distribution (called ‘calculation bands’ [4] or ‘columns’ [9]), allowing to consider longitudinal variations of the magnetic flux density along the cable length. A complete set of equations is written for all the columns, applying Faraday’s laws to the N-1 loops of each column. The cross over currents in each column can be calculated step by step from the knowledge of the cross over currents in the previous column [9]. The matrix approach, described in detail in [10] consists in expressing this relation in a matrix form.

In [9] it was shown that the Morgan's solution is only a particular solution of the general system of equations, which can be obtained imposing that the cross over currents of a certain column are all equal to the corresponding cross over currents of the previous column. Instead, a general solution of the system equations is characterised by the fact that the cross over currents of the $(k+N)^{th}$ column are equal to those of the k^{th} column, where k is the index of the column. This means that the cross over currents between any two strands of the cable are the same after every pitch length. The effects of sinusoidal distributions of the magnetic field along finite cables samples was analysed in [11], with the conclusion that the eddy currents distribution is pseudo-periodic if the period of the magnetic field oscillations exactly coincides with the cable twist pitch, and is periodic in the other cases.

In [4] the network model was applied to the study of the generation and development of the BICC's, due to longitudinal variations of the cross contact resistances or of the magnetic field perpendicular to the broad face of the cable, obtaining a good agreement with experimental data.
The network model describes in great detail every cross contact between the strands of the two layers, and gives local information about the currents flowing in every strand and in the cross contact resistances, and the power dissipated in the cable. It can take into account variations of the cable parameters across the cable width and simulate the generation and the development of short and long range coupling currents. The main drawback of this model is that the number of unknowns is very high, growing quickly with the cable size. This makes it very difficult to study the problem of current distribution in real long cables made of some tens of strands used in superconducting accelerator magnets. Moreover, one needs to include a fit parameter (the strand effective resistivity) in order to match the experimental data [4].

To overcome these drawbacks, we have developed a complete “continuum model” of multistrand superconducting cables [14, 15].
Our aim in the present work is to model correctly and in an optimised way the time dependent long range coupling currents, neglecting an accurate evaluation of the short range coupling currents. The way to calculate the steady state “supercurrents” in multistrand cables was suggested in [5]. The approach adopted there was to compute the total flux linked to two generic strands as the product of the area of the elementary loop formed by the two strands and the local value of the magnetic flux density. The steady state current in each strand can then be calculated considering the N-1 contributions given by the driving voltages induced in the loops formed by the strand considered and all the others. If the magnetic flux density change is applied to more than one loop a superposition of the effects of the different loops is calculated and the final currents in the strands are found.

The difficulty increases when all the cable strands are considered together, and the mutual dynamic interactions of the strand currents are taken into account to evaluate their time dependence. A simplified modelling of this situation was proposed in [16], where a single strand is considered and all the rest of the cable is lumped in another idealised strand, with which the current exchange takes place. An equivalent inductance of the strand and of all the rest of the cable, as well as an equivalent conductance between these two elements is evaluated, and the equation of current diffusion between the strand and the rest of the cable is then solved.

In this paper we introduce a complete “continuum” representation of the Rutherford cables, based on a distributed parameters circuit. In the next sections the model is developed and applied to the calculation of the current distribution in the presence of different longitudinal profiles of the magnetic flux density perpendicular to the cable axis.

2. Model description

2.1. Equations of the model

The model assumes that each strand carries a current distributed in a uniform way in its cross section, neglecting the influence of interfilament coupling currents flowing inside each strand between different superconducting filaments. We also assume that the current transfer between different strands happens along the length of the cable in a continuous manner. Under these assumptions we can derive approximate equations governing the current distribution in the cable.

To do so, we consider a superconducting cable made by N strands, and we examine the elemental length dx. Over this length the strands have parallel resistances $R_i = r_i\, dx$, (i=1, N), where r_i are the longitudinal resistances per unit length of cable (zero if the strand is in the superconducting state). The self inductances of the strands are indicated with $L_{ii} = l_{ii}\, dx$ where l_{ii} *(i=1,N)* are artificial parameters which we temporarily introduce. In the final equations only differences between these parameters appear, which have the physical meaning of per unit length induction coefficients. Finally, each strand can have an external voltage source $V^{ext}_i = v^{ext}_i\, dx$, that can be originated, for instance, by changes of the magnetic field flux due to external sources linked to a couple of strands. This idealised situation is represented schematically in Fig. 2.

The strands have initial currents i_i and voltages V_i at the coordinate x. Over an elemental length dx the currents will change by di_i because of the current transfer through the interstrand contact resistances $R_{hk} = 1/(g_{hk}\, dx)$, where g_{hk} is the interstrand conductance per unit length. Similarly the voltages will drop by dV_h due to the parallel resistance, inductance and the voltage source. Applying the Kirchhoff's current law to the N nodes, we obtain the following N dependent equations for the current variations:

$$\begin{cases} di_1 = -(g_{12} + g_{13} + ...g_{1N})\, dx\, V_1 + g_{12}\, dx\, V_2 + g_{13}\, dx\, V_3 ..... + g_{1N}\, dx\, V_N \\ di_2 = +g_{21}\, dx\, V_1 - (g_{21} + g_{23} + ...g_{2N})\, dx\, V_2 + g_{23}\, dx\, V_3 ... \quad ..... \quad + g_{2N}\, dx\, V_N \\ di_N = +g_{N1}\, dx\, V_1 + g_{N2}\, dx\, V_2 + g_{N3}\, dx\, V_3 .. \quad .- (g_{N1} + g_{N2} + ...g_{N\,N-1})\, dx\, V_N \end{cases} \tag{1}$$

where V_h is the voltage of strand h at position x.

Applying the Kirchhoff's voltage law to evaluate the voltage drops along the elemental mesh identified, and neglecting the inductive coupling for all sections, but for the one of length dx located at x, we obtain the following equations:

$$dV_h = v_h^{ext} dx - i_h r_h dx - \sum_{k=1}^{N} l_{hk} dx \frac{\partial i_k}{\partial t} \qquad h = 1,N \tag{2}$$

In addition, the solution is subject to a condition that expresses the conservation of the total operation current $i_{op}(t)$ in the cable cross section. We can write this condition as:

$$\sum_{h=1}^{N} i_h = i_{op}(t) \tag{3}$$

that must hold at any point in time and space. The equations above can be conveniently put in the following matrix form to ease the further algebra:

$$\frac{\partial \mathbf{v}}{\partial x} = -\mathbf{r}\mathbf{i} - \mathbf{l}\frac{\partial \mathbf{i}}{\partial t} + \mathbf{v}^{ext} \tag{4a}$$

$$\frac{\partial \mathbf{i}}{\partial x} = \mathbf{g}\,\mathbf{v} \tag{4b}$$

where we have defined the following vectors and matrices:

$$\mathbf{v} = \begin{bmatrix} V_1 \\ V_2 \\ \vdots \\ V_N \end{bmatrix} \;;\; \mathbf{i} = \begin{bmatrix} i_1 \\ i_2 \\ \vdots \\ i_N \end{bmatrix} \;;\; \mathbf{v}^{ext} = \begin{bmatrix} v_1^{ext} \\ v_2^{ext} \\ \vdots \\ v_N^{ext} \end{bmatrix} \tag{5a}$$

$$\mathbf{r} = \begin{bmatrix} r_1 & 0 & \cdots & 0 \\ 0 & r_2 & \cdots & 0 \\ \vdots & & & \\ 0 & 0 & \cdots & r_N \end{bmatrix} \;;\; \mathbf{l} = \begin{bmatrix} l_{11} & l_{12} & \cdots & l_{1N} \\ l_{21} & l_{22} & \cdots & l_{2N} \\ \vdots & & & \\ l_{N1} & l_{N2} & \cdots & l_{NN} \end{bmatrix} \;;\; \mathbf{g} = \begin{bmatrix} -\sum_{\substack{k=2 \\ k\neq 1}}^{N} g_{1k} & g_{12} & \cdots & g_{1N} \\ g_{21} & -\sum_{\substack{k=1 \\ k\neq 2}}^{N} g_{2k} & \cdots & g_{2N} \\ \vdots & & & \\ g_{N1} & g_{N2} & \cdots & -\sum_{\substack{k=1 \\ k\neq N}}^{N} g_{Nk} \end{bmatrix} \tag{5b}.$$

If we calculate the space derivative of equation (4b) assuming that the interstrand conductances are uniform along the cable axis, so that the spatial derivative of the interstrand conductances matrix **g** is nil, we obtain the following differential equations for the currents in the strands:

$$\mathbf{g}\mathbf{l}\frac{\partial \mathbf{i}}{\partial t} + \frac{\partial^2 \mathbf{i}}{\partial x^2} + \mathbf{g}\mathbf{r}\mathbf{i} - \mathbf{g}\mathbf{v}^{ext} = 0 \tag{6}$$

These are parabolic differential equations that describe the processes of current diffusion along the cable. The *N* equations in system (6) are linearly dependent, due to the application of the Kirchhoff's current law to all the nodes of the distributed circuit in the elemental mesh of length *dx*. However we can arbitrarily consider *N*-1 equations for the currents in the first *N*-1 strands and couple them to equation (3). In this way we obtain a complete set of *N* independent partial differential equations for the currents in the strands at any time and position:

$$\begin{cases} (gl)_{1,1}\dfrac{\partial\, i_1}{\partial t}+\cdots+(gl)_{1,N}\dfrac{\partial\, i_N}{\partial\, t}+(gr)_{1,1}\, i_1+\cdots+(gr)_{1,N}\, i_N+\dfrac{\partial^2 i_1}{\partial\, x^2}-(gv)_1^{ext}=0 \\ (gl)_{2,1}\dfrac{\partial\, i_1}{\partial t}+\cdots+(gl)_{2,N}\dfrac{\partial\, i_N}{\partial\, t}+(gr)_{2,1}\, i_1+\cdots+(gr)_{2,N}\, i_N+\dfrac{\partial^2 i_2}{\partial\, x^2}-(gv)_2^{ext}=0 \\ \vdots \\ (gl)_{N-1,1}\dfrac{\partial\, i_1}{\partial t}+\cdots+(gl)_{N-1,N}\dfrac{\partial\, i_N}{\partial\, t}+(gr)_{N-11}\, i_1+\cdots+(gr)_{N-1,N}\, i_N+\dfrac{\partial^2 i_{N-1}}{\partial\, x^2}-(gv)_{N-1}^{ext}=0 \\ \sum_{h=1}^{N} i_h = i_{op} \end{cases} \qquad (7)$$

where we indicate with $(gl)_{i,\,j}$ the element i, j of the result of the matrix product **gl**. These equations are in general not linear because the strand resistance depends on the current flowing in the strands, so that an appropriate model for the strand behaviour has to be chosen. Finally the appropriate length for the smearing of the system parameters (resistance, inductance and external voltage) has to be chosen. As multistrand superconducting cables have an intrinsic periodicity related to the twist pitch, good choices of the length for the smearing of electric parameters are appropriate multiples or fractions of the pitch. Once the parameters for matrices **g** and **l** are experimentally evaluated or calculated, the finite element method can be applied to solve system (7). The equations of the model developed in [7] for a two strands cable can be easily derived as a particular case of system (6).

2.2. Initial conditions

In order to solve system (7) by means of the finite element method it is necessary to fix the initial current distribution among the cable strands. The only physical situation in which a clear condition on strand currents can be set is at zero total current before any current ramp, when the following initial conditions hold:

$$i_h\,(x,0)=0 \qquad h=1,N \qquad (8).$$

A simple way to obtain this condition with a real magnet is to make it quench, so that the long "memory" of persistent currents flowing in the strands can be erased. In other cases, after a sufficiently long time from the last operation current variation, a simply resistive current distribution is established between the strands. As a starting point for the calculations, it can be assumed that the initial current distribution is uniform, i. e.:

$$i_h\,(x,0)=\frac{i_{op}(0)}{N} \qquad h=1,N \qquad (9)$$

2.3. Boundary conditions

The choice of the correct boundary conditions is quite delicate. In fact, in order to correctly model the connection of a multistrand superconducting cable to another cable through a termination or to a current lead through a joint, it would be necessary to have a complete description of the whole system (joint + cable + joint). However,

two reasonable choices of boundary conditions can be identified, which describe different properties of the actual cable end surfaces. If we consider the end surfaces to be equipotential, we can write:

$$v_h\,(x,0) = v_{h+1}\,(x,0) \qquad h = 1, N-1 \quad x = 0,\ x = L \tag{10}$$

This condition implies that the voltage differences between all the strands and strand N are nil:

$$e_h\,(x,0) = 0 \qquad h = 1, N-1 \quad x = 0,\ x = L \tag{11}$$

where we have defined:

$$e_h\,(x,t) = v_h\,(x,t) - v_n\,(x,t) \tag{12}$$

Applying the method of analysis based on nodes potentials, we can write system (4b) in terms of the voltage differences e_h (h= 1, N), obtaining a set of N-1 independent equations:

$$\begin{cases} -\dfrac{\partial i_1}{\partial x} = \left(g_{12} + g_{13} + \ldots\ldots g_{1N}\right) e_1 - g_{12} e_2 \ldots\ldots\ldots - g_{1N-1} e_{N-1} \\ -\dfrac{\partial i_2}{\partial x} = -g_{12} e_1 + \left(g_{21} + g_{23} + \ldots\ldots g_{2N}\right) e_2 \ldots\ldots\ldots - g_{2N-1} e_{N-1} \\ \vdots \\ -\dfrac{\partial i_{N-1}}{\partial x} = -g_{1N-1} e_1 - g_{2N-1} e_2 \ldots + \left(g_{1N-1} + g_{2N-1} + \ldots\ldots g_{N\,N-1}\right) e_{N-1} \end{cases} \tag{13}$$

The possibility to invert system (13) guarantees that a condition equivalent to (10) can be written for the space derivatives of the longitudinal currents in the strands:

$$\frac{\partial i_h}{\partial x} = 0 \quad h = 1, N-1 \quad x = 0,\ x = L \tag{14}$$

As the operation current is only a function of time, from equation (3) it can be deduced that the condition (14) holds for the N^{th} strand as well, so that the complete boundary conditions in the equipotential end surfaces case can be written as:

$$\frac{\partial i_h}{\partial x} = 0 \quad h = 1, N \quad x = 0,\ x = L \tag{15}$$

Another possibility is to assume that the current distribution is uniform at the cable ends, imposing the following boundary conditions:

$$i_h(x,\,t) = \frac{i_{op}(t)}{N} \quad h = 1, N \quad x = 0,\ x = L \tag{16}$$

Different kinds of boundaries can in principle be described by an accurate choice of the model parameters at the cable ends.

2.4. Contact conductances per unit length

In order to define the smeared interstrand conductances, we consider that each strand crosses every other strand in two points per twist pitch. Indicating with $R^c_{h,k}$ the interstrand cross contact resistance between strand *h* and strand *k*, and with L_p the cable twist pitch, the cross contact conductance per unit length is given by the following expression:

$$g^c_{h,k} = \frac{2}{L_p R^c_{h,k}} \tag{17}$$

The description of the cross contact resistance between strands given by the network model is closer to the physical reality of the cross contacts than that given by the continuum model, while a better representation of the contact between adjacent strands is given by the present model.

However, in order to make comparisons with the network model, and to consistently calculate the interstrand adjacent conductances, we consider that in the most advanced versions of the network model [4, 10], a lumped contact resistance $R^a_{h,k}$ is inserted between two adjacent strands at the same positions in which they have cross contacts with the strands of the other layer. Every strand crosses all the other strands in two points per twist pitch, so that a total of 2 (*N*-1) lumped resistances are inserted along a twist pitch between each pair of adjacent strands. The equivalent adjacent conductance per unit length results in:

$$g^a_{h,k} = \frac{2\,(N-1)}{R^a_{h,k} L_p} \tag{18}$$

2.5. Mutual inductances matrix

For the calculation of the matrix of mutual inductances we assume the current density to be uniform inside each strand. The strands are considered to be made of straight cylinders layered alternatively in the upper and lower face of the cable. Starting from a generic position along the cable axis we consider all the cylinders of each strand within a certain number of cable pitches, in order to smear the periodic variations of the inductances matrix along the cable axis.

If we consider *p* pitches of cable the total number of cylinders for each strand introduced in the calculations is equal to 2*p* or 2*p* + 1, depending on the strand chosen. As an example, the cylinders considered for the calculation of the mutual inductances matrix for strand 1 (2 cylinders) and strand 3 (3 cylinders) in the case of a calculation for 1 pitch are shown in Fig. 1. The mutual inductance between a generic cylinder *i* of

strand *h* and a generic cylinder *j* of strand *k* is calculated by means of an adaptive recursive numerical integration of the following formula:

$$M_{h,i,k,j} = \frac{1}{\Omega_s \Omega_s} \frac{\mu_0}{4\pi} \int_{V_{h,i}} \int_{V_{k,j}} \frac{\mathbf{u}_{h,i}(\mathbf{x}') \cdot \mathbf{u}_{k,j}(\mathbf{x})}{|\mathbf{x}-\mathbf{x}'|} d^3\mathbf{x}' d^3\mathbf{x} \tag{19}$$

where Ω_s is the area of the strand cross section, μ_0 is the permeability of vacuum, $\mathbf{u}_{h,i}$ and $\mathbf{u}_{k,j}$ are unit vectors tangent to the axis of the strands, and $V_{h,i}$, $V_{k,j}$ are the volumes of the strands segments. Once the mutual inductances between all the strand sectors are known, the elements of the matrix of the self and mutual inductances per unit length can be calculated as follows:

$$l_{h,k} = \frac{\sum_{i=1}^{C(h)} \sum_{j=1}^{C(k)} M_{h,i,k,j}}{pL_P} \tag{20}$$

where $C(h)$ is the number of cylinders owing to strand *h* along the *p* pitches considered. It is worth remarking that the absolute values of the mutual induction coefficients change with the number of cable pitches chosen for the smearing. However, only differences between these coefficients appear in the final equations in the matrix ***gl***. We have verified that the elements of matrix ***gl*** are quickly convergent with the number of pitches, obtaining a constant value within 6 - 7% after 10 twist pitches. As we are interested to study effects that involve many twist pitches (up to the whole cable length), we believe that in general these variations do not affect substantially the final current distribution, and we have verified it in the test cases reported in the following sections.

2.6. Longitudinal resistance

The strand longitudinal resistance is in general dependent on the magnetic flux density ***B***, on the temperature *T*, and on the current flowing in the strand. Once the longitudinal resistance per unit length of the strand $r_{s,h}$ is known, the longitudinal resistance per unit length of cable r_h can be found as:

$$r_h(x) = \frac{r_{s,h}}{\sin\alpha} \tag{21}$$

where α is indicated in Fig. 1.

2.7. External voltage per unit length

The external voltage per unit length can be defined in the following way:

$$v_h^{ext}(x,t) = -\frac{\partial \mathbf{A}^{ext}}{\partial t}(x,y,z,t)\cdot \mathbf{u}_h(x) \qquad (22)$$

where $\mathbf{A}^{ext}$ is the magnetic vector potential associated with the external sources, $\mathbf{u}_h$ is the unit vector tangent to the axis of strand *h*. This definition guarantees that the integral effect of the difference v^{ext}_h - v^{ext}_k along any loop formed by two generic strands *h* and *k* provides a driving force equivalent to the time derivative of the magnetic flux linked to the loop.

3. Comparison with the network model

We have applied the model to the evaluation of currents induced by longitudinal variations of the external field perpendicular to the broad face of the cable. A comparison between the results obtained with the continuum and the network model illustrated in [4] is shown in Fig. 3 in the case of a simple step variation of the magnetic field along the cable axis. As far as possible the same conditions as in [4] have been used for the simulations. The cable considered is a 16 strands cable, with $R^c_{h,k}$ = 1 μΩ, $R^a_{h,k}$ = 10 μΩ for every *h* and *k* and L_p = 100 mm. The cable is exposed to a time dependent magnetic field perpendicular to its broad face equal to 0 for $x < L/2$ and increasing with a rate of 0.01 T/s for $x > L/2$. It was assumed in [4] that the strand can be characterised by a constant and uniform longitudinal effective strand resistivity. For the sake of comparison, we have introduced a uniform and constant longitudinal resistance per unit length r_h, and we have evaluated the strand currents at the final steady state for two different values of r_h, equal to 1.54 10^{-8} Ω/m and 1.54 10^{-11} Ω/m.

In the case reported in Fig. 3 the short range coupling currents due to the uniform field applied at the right of $x = L/2$ are superimposed to the main long range coupling currents due to the field variation at $x = L/2$. It can be noticed that the qualitative behaviour of the BICC's obtained with the two models is very similar in both the current distribution regimes shown. Only a quantitative difference in the range 5-20% on the maximum amplitude of the BICC's is found. This could be due to the slightly different description of the geometry of the cable made in the two models. The present model in fact is based on the simple geometry illustrated in Fig. 1, with a discontinuous jump of the strands from one layer to the other. In the model described in [4] instead, the strands go from one layer to the other via short side cylinders.

In the evaluation of the short range coupling currents, instead, the two models strongly differ. In fact, the amplitude of these currents obtained with the continuum model is about half of that obtained through the network model. This is due to the smearing of the system parameters performed in the continuum model and can be confirmed by an analytical calculation of the short range coupling currents in the simple case of a two strand cable made of an integer number of pitches to which an uniform time dependent magnetic field is applied.

As anticipated in the introduction, our aim here is to model correctly the behaviour of the long range coupling currents, neglecting the influence of short range coupling

currents. For this reason we have tried to find the minimum number of mesh points needed for a correct evaluation of the long range BICC's. We have found that with 2 mesh points per pitch the main BICC's can be very well approximated for the case-study previously described (see Fig. 4). If the longitudinal variations of the time derivative of the field were less sharp, appropriate meshing strategies could lead to even larger meshes.

Considering that in the network model there are (5N-3) unknowns per calculation band, and N bands per pitch, we end up with a total of (5N-3)·N unknowns per pitch. In the actual implementation of the continuum model a point collocation method [17] has been used for the numerical solution of system (7), with two gaussian points per elemental mesh. This results in a total of $2M_PN$ unknowns per pitch, where M_P is the number of mesh points per pitch. The ratio of the number of unknowns per pitch of cable in the two models is then equal to:

$$\Re = \frac{5\,(N-3)}{2\,M_P} \tag{23}$$

In the case reported in Fig. 4 $\Re$ is approximately equal to 16. This leads to a remarkable computational advantage, which allows the application of the continuum model to the study of real long Rutherford cables operating in accelerator magnets.

4. Comparison with experimental data

We have applied the continuum model to the evaluation of BICC's in the inner layer cable of a short LHC dipole model. This dipole has been extensively measured to evaluate the dependence of the amplitude of the periodic oscillations of the magnetic field in the magnet bore (called "magnetic field periodic pattern") on the powering history of the magnet [18].

The coil has two poles assembled from an inner and an outer layer. The inner layer of a single pole is wound from 15 turns arranged into 3 blocks, while the outer layer has 26 turns arranged in 2 blocks corresponding to different angular positions, as shown in Fig. 5. The layers in a pole are wound individually, and the cable ends are either soldered together at the interconnection between layers and poles or connected through splices to the current leads. We assume that the magnetic field pattern is only related to the current distribution in the inner layer cable, because the periodicity of the field oscillation is exactly coincident with the inner layer cable twist pitch. We have simulated the current diffusion in the upper pole part of the inner layer cable. This part of cable is made of 28 strands, with a total length of 27.8 meters, a twist pitch of 115 mm., and a thickness of 1.88 mm. The cable has been exposed to current cycles made of a linear ramp up + plateau, with different ramp rates and flat top currents.

In order to simulate the current distribution during these cycles, we have calculated with ROXIE [19] the magnetic field perpendicular to the broad face of the cable. We have considered for the simulations the average value of the field across the cable

width, neglecting the field variations in the y direction, and we have applied it along the developed length of the cable axis. Moreover, we have taken the field proportional to the total current in the magnet, neglecting the iron saturation at high magnetic fields.

The results of simulations are reported in Fig. 6 for a current step with a ramp rate of 50 A/s and a final current of 2000 A. The magnetic field perpendicular to the cable face shows strong, short range longitudinal variations due to the cable bending over the magnet bore. It can be noticed that soon after the beginning of the ramp sharp current spikes appear in these regions of high field gradient (Fig. 6a). At the end of the field ramp the correspondence between the field profile and the current pattern is less evident (Fig. 6b). After 1000 s from the beginning of the current flat top, we note a remarkable current difference between the strand currents, but the correspondence with the field profile is lost (Fig. 6c).

In order to compare the calculated and measured results, we assume that the amplitude of the magnetic field periodic pattern is proportional to the differences between the currents flowing in the strands. In particular we take the values of the maximum difference between the strand currents in the middle of the uniform field regions, ΔI_{max}, as a reference quantity for a qualitative comparison with the amplitude of the magnetic field pattern measured outside the cable next to these positions.

In Fig. 7 we compare the amplitude of magnetic field pattern at position A in the cross section (r = 17 mm. and $\theta = 35°$, Fig. 5) and parameter ΔI_{max} calculated for turn 7-a which faces the point selected. The behaviour of the amplitude of the pattern is qualitatively similar to that of the maximum current difference, both respecting the typical feature of the response to current steps shown by a two strand cable in a much simpler situation [7].

This qualitative agreement is reinforced by the fact that the measured amplitude of magnetic field pattern at the end of the ramps, and the calculated values of ΔI_{max} at the same time, show the same kind of dependence on the current ramps parameters. These two quantities are in fact linearly dependent on the final flat top current and approximately independent on the ramp rate.

5. Conclusions

A continuum representation of superconducting Rutherford cables has been developed for the evaluation of long range eddy currents generated by time dependent magnetic fields applied to the cable. The results on the current distribution pattern are in good agreement with those obtained with a network model of the cable in the case of a simple step-like distribution of the magnetic field perpendicular to the cable axis. The computational advantages of the present model allow to simulate the current distribution in real long cables used in magnets. A qualitative agreement between the results on current distribution in the inner cable of an accelerator dipole and the experimental data on the magnetic field pattern generated inside the magnet bore has been obtained.

References

[1] M. N. Wilson. Superconducting Magnets. Oxford: Oxford University Press, 1983.

[2] W. J. Carr. AC Loss and Macroscopic Theory of Superconductors. New York: Gordon and Beach, 1983.

[3] V. A. Altov, V .B. Zenkevitch, M. G. Kremlev, V. V. Sytchev. Stabilization of Superconducting Magnetic Systems. New York: Plenum, 1973.

[4] A. P. Verweij. Electrodynamics of Superconducting cables in Accelerator Magnets. Ph.D. Thesis, 1995; University of Twente, Enschede, (NL).

[5] L. Krempasky, C. Schmidt. Theory of "supercurrents" and their influence on field quality and stability of superconducting magnets. Jour.Appl. Phys., 1995; 78 (9).

[6] L. Krempasky, C. Schmidt. Ramp rate limitation in large superconducting magnets due to 'supercurrents'. Cryogenics, 1996; 36 (6): 471

[7] L. Krempasky, C. Schmidt. Experimental verification of 'supercurrents' in superconducting cables exposed to AC fields. Cryogenics, 1999; 39: 23.

[8] G.H. Morgan. Eddy currents in flat metal-filled superconducting braids. Jour. Appl. Phys., 1973; 44 (7): 3319.

[9] A.A. Akhmetov, A. Devred, T. Ogitsu. Periodicity of Cross-over Currents in a Rutherford-type Cable Subjected to a Time Dependent Magnetic Field. Jour. Appl. Phys., 1994; 75 (6): 3176.

[10] A. Akhmetov. Network models of superconducting cables and the results of the matrix approach to their description. Physica C, 1998; 310: 309.

[11] A. Akhmetov, K. Kuroda, K. Ono and M. Takeo. Eddy currents in flat two-layer superconducting cables. Cryogenics 1995; 35: 495.

[12] A. Akhmetov, K. Kuroda, T. Koga, K. Ono and M. Takeo. Decay of long current loops in the superconducting cables. Proceedings of EUCAS'95, 1995, Scotland.

[13] A. P. Verweij, H.H.J. ten Kate. Super Coupling Currents in Rutherford Type of Cables due to longitudinal Non-homogeneities of dB/dt. IEEE Trans. Appl. Sup., 1995; 5 (2): 404.

[14] L. Bottura. Modelling stability in superconducting cables. Physica C, 1998; 310: 316.

[15] L. Bottura, M. Breschi, F. Negrini, P.L. Ribani. Electromagnetic analysis of current distribution in multistrand superconducting cables. Inst. Phys. Conf. Ser., 2000; 167: 1191.

[16] A. Akhmetov, A. Devred, R. Mints, R. Schermer. Current Loop Decay in Rutherford Type Cables. Supercollider, 1993; 5: 443.

[17] N. K. Madsen, R. F. Sincovec. ACM Trans. on Mathematical Software. 1979; 5: 326.

[18] L. Bottura, M. Breschi, M. Schneider. Measurements of Magnetic Field Pattern in a Short LHC Dipole Model. Paper 1LH01, presented at ASC 2000, Virginia Beach, September 2000.

[19] In: Proc. First Int. ROXIE users meeting, Geneva, S. Russenschuck ed., 1999, Cern Report 99-01.

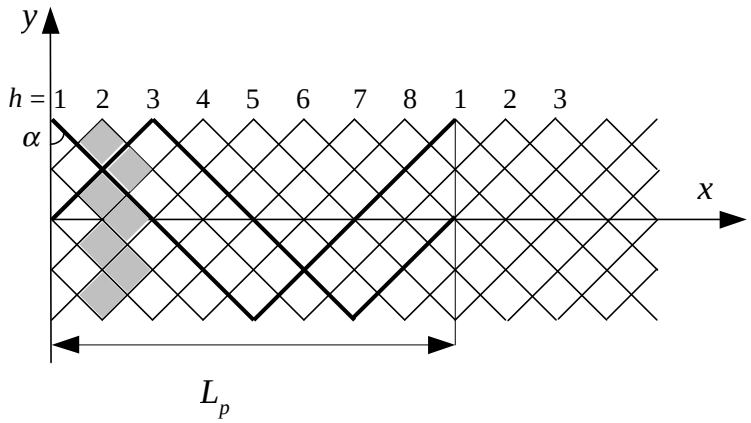

Fig. 1 Top view of the idealised geometry of the strand axes of a Rutherford cable used for the continuum model. The thick lines represent the strand segments of strand 1 and 3 considered for the calculation of the mutual inductances matrix along one pitch. The shaded areas represent the *N*-1 loops used in Morgan's network model, and as elemental calculation bands in the following versions of the network model.

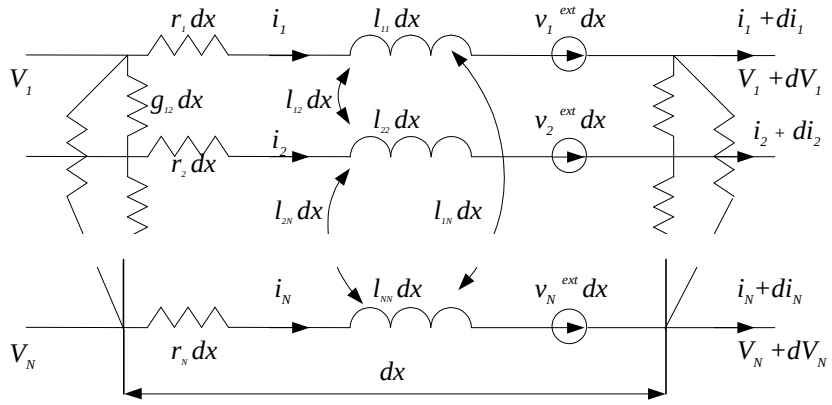

Fig. 2 Distributed circuit model of the elemental mesh of cable used in the continuum model

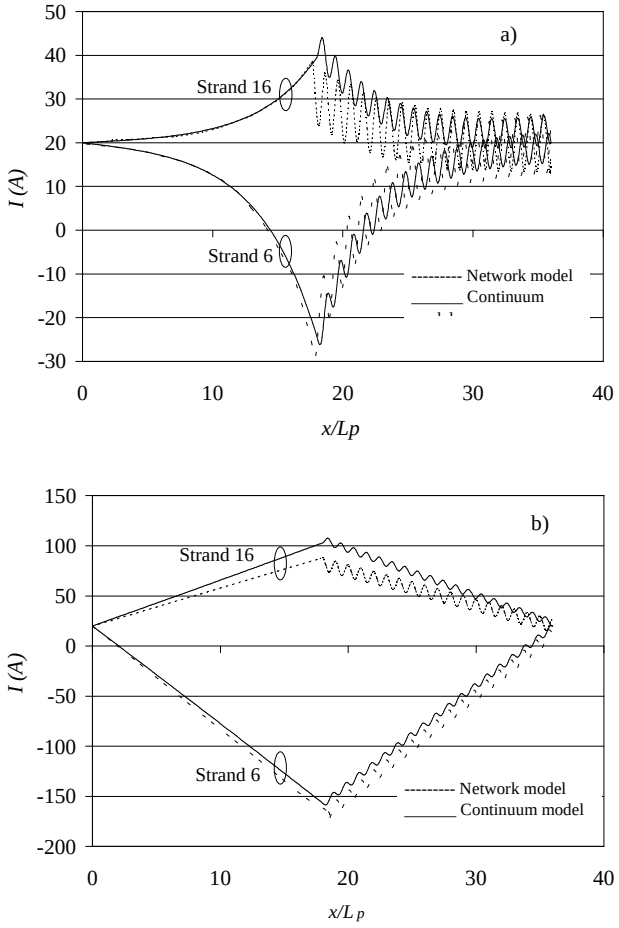

Fig. 3 Comparison between network and continuum model: behaviour of Boundary Induced Coupling Currents in a 16 strands Rutherford cable at the regime condition in the case of a step-like spatial distribution of the magnetic flux density perpendicular to the broad face of the cable. a) r_h = 1.54 10^{-8} Ω/m b) r_h = 1.54 10^{-11} Ω/m.

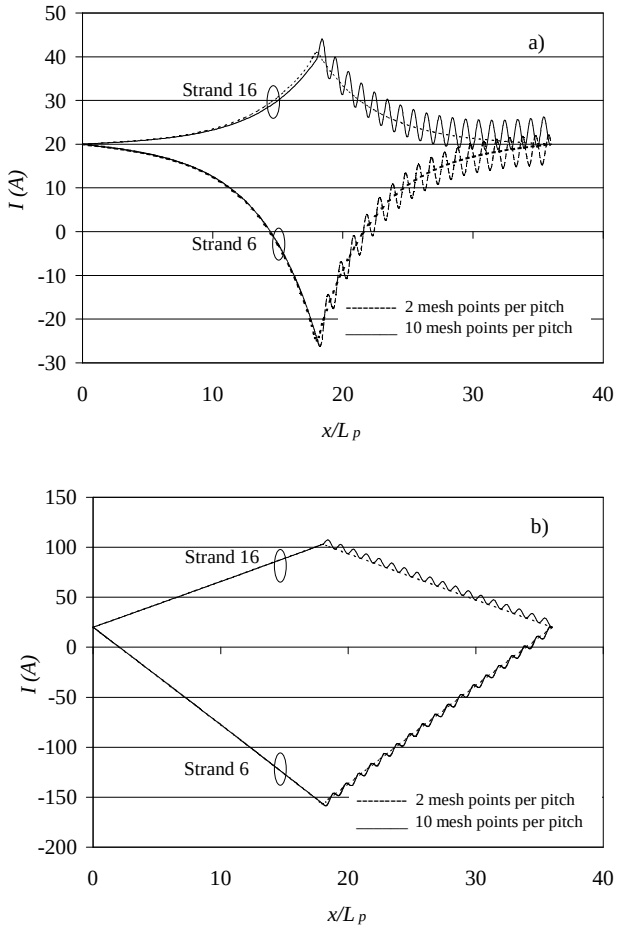

Fig. 4 Comparison between two different calculations performed with the continuum model in the same cases reported in Fig. 3. The two calculations are performed with a different number of mesh points per pitch, showing that the main BICC's can be well described with only two mesh points per pitch.

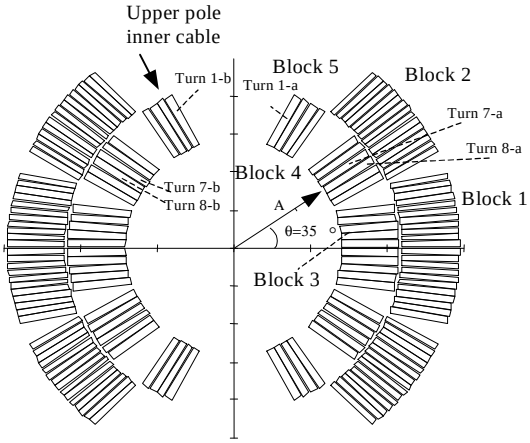

Fig. 5 Cross section of one aperture of the double aperture dipole model MBSMT1 used in the experiments.

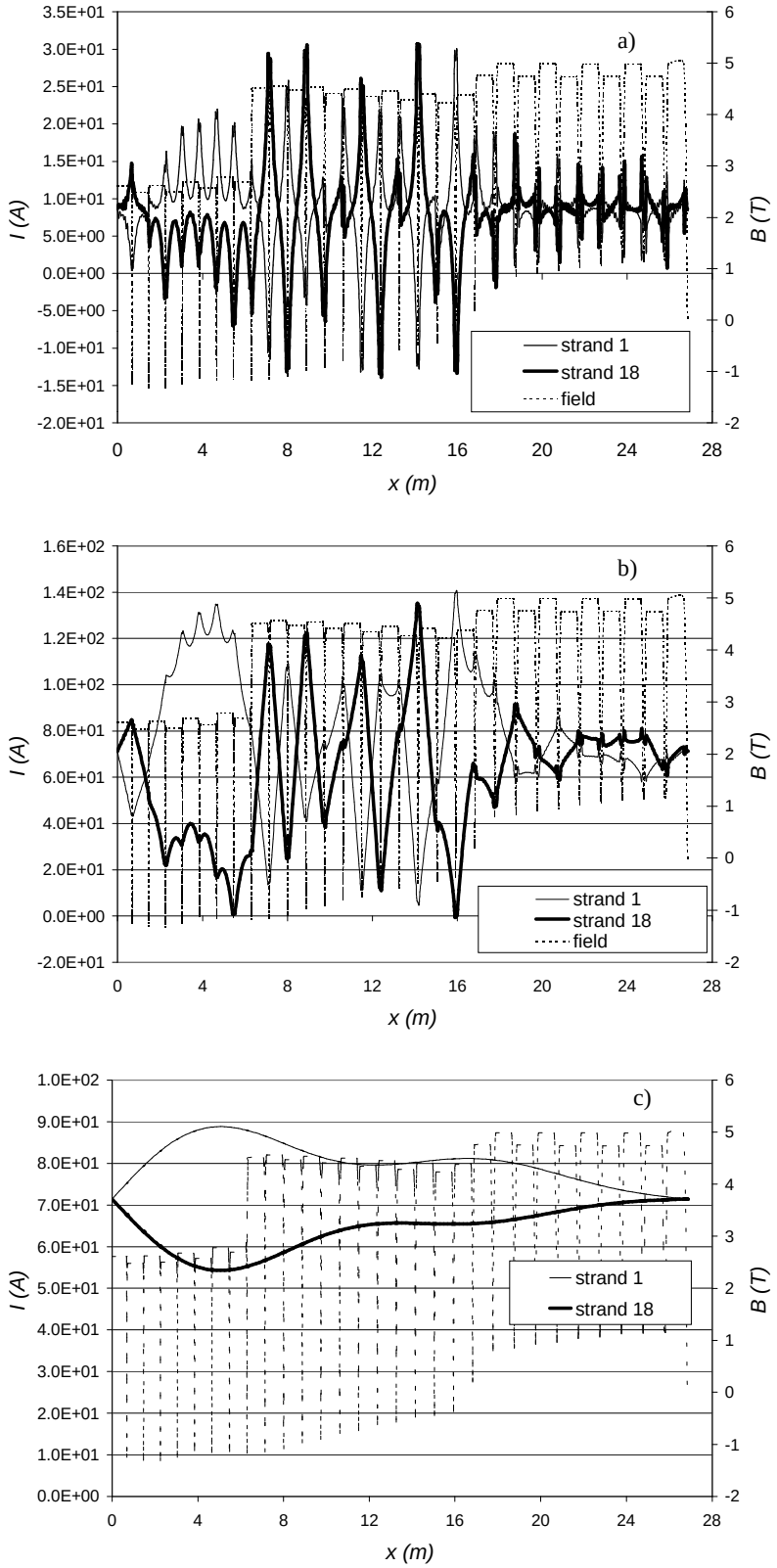

Fig. 6 Behaviour of the currents in two strands of the 28 strand cable along the cable length at different times. *RR* = 50 A/s I_{FT}= 2000 A a) t = 3.85 s (soon after ramp start) b) t=39 s (end of the ramp) c) t=1039 s (end of the plateau). The dotted line indicates the main background magnetic field perpendicular to the cable axis calculated at i_{OP} = 11500 A.

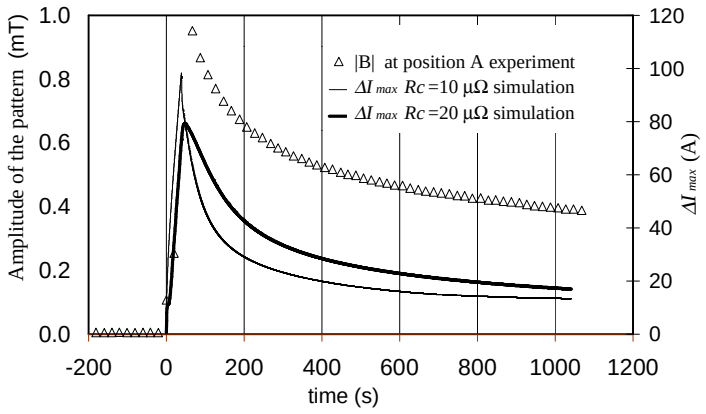

Fig. 7 Comparison between the time evolution of the amplitude of the periodic pattern in the middle of the uniform field region and that of parameter ΔI_{max} calculated at turn 7-a. Time t is set to zero at the beginning of the current step, made of a linear increase up to 2000 A with a ramp rate of 50 A/s and a flat top of 1000 s at the maximum current.